Journal of Alloys and Compounds, *187* (1992) 39–48
JALCOM 308

The crystal structure of defective $YAlB_{14}$ and $ErAlB_{14}$

M. M. Korsukova*, T. Lundström and L.-E. Tergenius
Institute of Chemistry, Box 531, S-751 21 Uppsala (Sweden)

V. N. Gurin
A. F. Ioffe Physical-Technical Institute, Academy of Sciences of Russia,
194021 St Petersburg (Russian Federation)

(Received Feburary 4, 1992)

Abstract

The crystal structures of $Y_{0.62}Al_{0.71}B_{14}$ and $Er_{0.62}Al_{0.73}B_{14}$ belong to the $MgAlB_{14}$-type structure. The refinements are based on the space group *Imma* and converged at the conventional *R* values 5.0% (2908 reflections) and 3.4% (2394 reflections) respectively. The cell dimensions of the single crystals are $a = 5.8212(3)$ Å, $b = 10.4130(8)$ Å, $c = 8.1947(6)$ Å and $a = 5.8200(1)$ Å, $b = 10.3950(4)$ Å, $c = 8.1825(3)$ Å respectively. Important structural characteristics are partial occupancy of both metal positions and a splitting of the rare earth atomic position.

1. Introduction

Recently, the preparation of single crystals of icosahedral borides with the general formula $LnAlB_{14}$ (Ln ≡ Tb, Dy, Ho, Er, Yb, Lu) was reported [1–3]. The crystals were obtained by high temperature solution growth from molten aluminium. Examination of these crystals by X-ray diffraction methods showed that they belong to the $MgAlB_{14}$-type structure (orthorhombic; space group, No. 74, standard setting *Imma*). An X-ray single-crystal diffractometry study has been performed only for the holmium compound [1, 3]. The crystal structure of $HoAlB_{14}$ was found to be essentially the same as that of $LiAlB_{14}$ [4], although partial occupancies were established for both the holmium and the aluminium sites. The refined composition of the crystal was $Ho_{0.63}Al_{0.74}B_{14}$. Partial occupancies for both metal sites were also found earlier in $MgAlB_{14}$ ($Mg_{0.78}Al_{0.75}B_{14}$). In addition, the magnesium site in this compound was split into two positions, situated 0.39 Å from each other [5].

The measurements of the magnetic and electrical properties of some of the new $LnAlB_{14}$ compounds showed that they represent a new group of magnetic semiconductors, displaying some formal resemblance to diluted magnetic semiconductors [2, 3]. In particular, to explain the giant negative magnetoresistance of $ErAlB_{14}$, the assumption of some kind of structural disorder in this compound had to be employed [3].

---

*On leave from A. F. Ioffe Physical-Technical Institute, Academy of Sciences of Russia, 194021 St Petersburg, Russia.

0925-8388/92/$5.00

2. Experimental details

2.1. Crystal growth

Crystals of $YAlB_{14}$ and $ErAlB_{14}$ were prepared by high temperature solution growth from aluminium melts [1, 3]. The nominal purities of the starting materials were 99.7–99.9 wt.%, better than 99 wt.% and 99.99 wt.% for the yttrium and erbium metals, amorphous boron powder and aluminium respectively. The initial boron-to-yttrium (or erbium) atomic ratio was 14 to 1 and the boron concentration in the aluminium solvent was 1.9 wt.%. The crystallization processes were carried out in alumina crucibles under an inert gas flow (argon). A vertical, resistively heated furnace was used. The mixtures were initially heated to 1400 °C, soaked at this temperature for 5 h and then slowly cooled to room temperature. The crystals were separated from the solidified matrix by dissolving the excess aluminium in diluted hydrochloric acid (1:3).

The crystalline products thus obtained were examined under an optical microscope. Crystals of the $MgAlB_{14}$-type phases were carefully selected by hand for further studies. The crystals displayed mainly three different morphologies: needle-like and plate-like crystals up to (1–3) mm × 1 mm × 0.5

TABLE 1

Crystal and diffraction data for $YAlB_{14}$ and $ErAlB_{14}$

	$Y_{0.62}Al_{0.71}B_{14}$	$Er_{0.62}Al_{0.73}B_{14}$
Space group	*Imma* (No. 74)	*Imma* (No. 74)
Cell dimensions (Å)	$a = 5.8212(3)$ $b = 10.4130(8)$ $c = 8.1947(6)$	$a = 5.8200(1)$ $b = 10.3950(4)$ $c = 8.1825(3)$
Crystal dimensions (μm^3)	210 × 123 × 131	165 × 139 × 88
Absorption coefficient (cm^{-1})	73.9	102.8
Number of boundary planes	13	14
Transmission factors	0.262–0.372	0.175–0.332
2θ limit (deg)	93.5	100.0
Number of reflections measured	2607	2989
Number of non-equivalent reflections	1247	1438
X-ray density ($g\ cm^{-3}$)	3.02	4.20

TABLE 2

Agreement indices for equivalent reflections before and after absorption correction

	R (R_w) (% (%))	
	Before correction	After correction
$YAlB_{14}$	5.06 (5.44)	3.35 (2.67)
$ErAlB_{14}$	5.33 (7.33)	2.52 (3.08)

mm in size and much smaller isometric crystals. The crystals had smooth faces with a metallic lustre, but very thin platelets were translucent and of deep-red colour.

2.2. *Intensity measurement*

Well-formed crystals of $YAlB_{14}$ and $ErAlB_{14}$ were used for the measurements of the X-ray diffraction intensities. These and the unit-cell dimensions were measured with an automatic four-circle diffractometer using graphite monochromated Mo Kα radiation ($\lambda = 0.710\ 73$ Å) and the ω–2θ scan technique. The stability of the primary X-ray beam and the equipment was checked by remeasuring five standard reflections at every sixtieth reflection. A long-term systematic decrease in intensity within the time period of measurement was observed for both crystals (approximately 1% for $YAlB_{14}$ and 2% for $ErAlB_{14}$), and a proper correction for this decrease was applied in the subsequent analysis. Crystal and diffraction data are presented in Table 1.

The intensity data were corrected for Lorentz and polarization effects. Absorption corrections were applied using the gaussian grid technique. The agreement indices for equivalent reflections before and after absorption correction are given in Table 2.

3. Refinements of structures

Refinements were carried out using the full matrix least-squares program DUPALS [6], which includes a correction procedure for extinction effects according to the theory of Becker and Coppens [7]. The values adopted for the atomic scattering factors and for the anomalous dispersion corrections were those given in ref. 8. The initial refinements were performed for the yttrium as well as the erbium compound using atomic coordinates and temperature factors from the holmium compound [1, 3] as starting parameters. The refinements converged at 18–20% for a refinement including variation in all positional and isotropic temperature factors and the occupancy factors for both metal atoms. Refinements using neutral and trivalent scattering factors for the metal atoms (yttrium, erbium and aluminium) were carried out. As a result it was found that the only difference between the two options was a slightly higher (by three to four standard deviations) occupancy for the metal positions when trivalent scattering factors were used. However, magnetization measurements have shown that the rare earth atoms adopt the trivalent state [2, 3] and therefore, in the final refinements, scattering factors for 3+ metal ions and neutral boron atoms were adopted.

Preliminary refinements showed that the isotropic extinction model is fully adequate for both crystals. Furthermore, it was found that the model of type II (crystal-size-dominated extinction) gives a better fit for the yttrium compound while the model of type I (mosaic-spread-dominated extinction) is more appropriate for the erbium compound. The reader is referred to ref. 7 for more details on extinction corrections.

In the refinements, attempts were included to refine the structure using the non-centrosymmetric space group *Im2a*, a non-standard setting of space group No. 46 in ref. 9. The result for $Er_{0.62}Al_{0.73}B_{14}$ was a significantly higher occupancy for one half-set of symmetry-related equivalent atoms (those with $x = -0.022\,54$) compared with the other half-set of the earlier centrosymmetrically related atoms (those with $x = 0.022\,54$). There was no significant difference as to the positional coordinates, however, and the refinement did not converge when all parameters were varied simultaneously owing to the very strong correlation between some of the parameters refined. The occupancy of the first-mentioned position was 33.2% while the occupancy of the second position was 28.7% (a difference of 17 standard deviations). The occupancy of the hole was 61.9% in the non-centrosymmetric refinement, which is very close to the 61.6% obtained using the centrosymmetric assumption. The R value obtained was significantly higher than those from the refinements carried out under the assumption of centrosymmetry. Because of these observations the centrosymmetric space group *Imma* was selected for the presentation of the structure.

The refinements were based on F^2 and in the final refinement the following parameters were varied for both structures: one scale factor, two occupancy factors, 14 positional parameters, five isotropic temperature factors, eight anisotropic temperature factors and one isotropic extinction parameter. The S values (standard deviations of an observation of unit weight [8]) were 1.10 and 0.99 for the yttrium and erbium compound respectively, which indicates that the weights used are satisfactory. Similarly, the slopes (1.10 and 1.12 respectively) and the y intercepts (-0.09 and -0.19 respectively) of the normal probability plots of the ranked weighted differences indicated a correct weighting. The final conventional R values were 0.050 (2908 reflections) and 0.034 (2394 reflections), the final $R(F^2)$ values were 0.050 (2394 reflections) and 0.047 (2908 reflections) while the final weighted $R_w(F^2)$ values were 0.078 and 0.074 for the erbium and yttrium compounds respectively. A final electron density and Fourier difference map was calculated for both structures. The largest peak in these maps corresponded to 2.5% and 3.3% of a boron peak for $YAlB_{14}$ and ErB_{14}, respectively. The final structure data have been collected in Tables 3 and 4 and the interatomic distances of the structures are presented in Table 5.

Recently, a charge density study on $LiAlB_{14}$, which is isostructural with the present two compounds, was reported. The study gave clear indications of a charge transfer from the metal atoms to the boron network. A similar study was therefore attempted for the most promising of the present two compounds, namely $YAlB_{14}$. This compound has a significantly higher value of the suitability index, defined as $V_{cell}/{n_{core}}^2$ (n_{core} is the number of core electrons) [10], namely 0.13, compared with 0.06 for the erbium compound. In the present study we reduced the influence of a non-spherical distribution of valence electrons by refining the structure using only large-angle reflections (1584 reflections with $(\sin\theta)/\lambda > 0.65$). A Fourier difference map was subsequently calculated using all observed structure factors and the corresponding

TABLE 3

Final structure data for $Er_{0.62}Al_{0.73}B_{14}$ and $Y_{0.62}Al_{0.71}B_{14}$, where the estimated standard deviations are given in parentheses (space group, *Imma* (No. 74))

Atom	Position	x	y	z	B_{iso} (Å^2)	Occupancy
$Er_{0.62}Al_{0.73}B_{14}$						
Er	8i	0.02372(5)	¼	0.64219(2)	Anisotropic	0.310(1)
Al	4c	¼	¼	¼	Anisotropic	0.732(4)
B(1)	8h	0	0.1663(1)	0.9683(1)	0.32(1)	1
B(2)	8h	0	0.1520(1)	0.3753(1)	0.38(1)	1
B(3)	8h	0	0.0877(1)	0.1702(1)	0.33(1)	1
B(4)	16j	0.1600(1)	0.05967(7)	0.83769(8)	0.31(1)	1
B(5)	16j	0.2484(1)	0.08008(7)	0.45538(8)	0.33(1)	1
$Y_{0.62}Al_{0.71}B_{14}$						
Y	8i	0.02511(8)	¼	0.64217(3)	Anisotropic	0.310(1)
Al	4c	¼	¼	¼	Anisotropic	0.708(3)
B(1)	8h	0	0.1660(1)	0.9682(1)	0.35(1)	1
B(2)	8h	0	0.1520(1)	0.3745(1)	0.39(1)	1
B(3)	8h	0	0.0882(1)	0.1704(1)	0.35(1)	1
B(4)	16j	0.1602(1)	0.05917(6)	0.83757(7)	0.34(1)	1
B(5)	16j	0.2482(1)	0.08028(6)	0.45487(8)	0.35(1)	1

TABLE 4

Anisotropic displacement parameters for $Er_{0.62}Al_{0.73}B_{14}$ and $Y_{0.62}Al_{0.71}B_{14}$ (displacement factor, $\exp(-2\pi^2\Sigma_i\Sigma_j U_{ij}h_ih_ja^*_ia^*_j)$)

Atom	U_{11} (Å^2)	U_{22} (Å^2)	U_{33} (Å^2)	U_{13} (Å^2)
$Er_{0.62}Al_{0.73}B_{14}$				
Er	0.0117(1)	0.00467(4)	0.00550(4)	0.00103(4)
Al	0.0108(3)	0.0047(3)	0.0190(3)	0.0105(3)
$Y_{0.62}Al_{0.71}B_{14}$				
Y	0.0087(2)	0.00446(8)	0.00466(8)	−0.00045(9)
Al	0.0112(3)	0.0053(2)	0.0196(3)	0.0108(2)

calculated structure factors, based on the parameters from the large-angle refinement. However, this difference synthesis did not deviate significantly from the previous one, the largest peak being 2.4% of a boron peak in the F_o synthesis. No further attempts to study the charge distribution was made, although it might be profitable to apply the population refinement method.

Crystals from the same batch as those used for the diffraction study were analysed using an electron microprobe (acceleration voltage, 20 kV). A total of three crystals and six crystals were analysed for the erbium and the yttrium compounds respectively, and a total of 12 points for each compound. No significant differences between different crystals were found,

TABLE 5

Interatomic distances in $Er_{0.62}Al_{0.73}B_{14}$ and $Y_{0.62}Al_{0.71}B_{14}$, where the distances listed are all M–M < 3.66 Å, M–B < 3.47 Å and B–B < 2.74 Å

Atoms	Distance (Å)		Atoms	Distance (Å)	
	RE≡Er	RE≡Y		RE≡Er	RE≡Y
RE–RE	0.276(1)[a]	0.292(1)[a]	B(1)–B(1)	1.739(2)	1.750(2)
–2B(2)	2.414(1)	2.424(1)	–2B(4)	1.800(1)	1.803(1)
–2B(4)	2.665(1)	2.670(1)	–2B(5)	1.827(1)	1.828(1)
–2B(5)	2.677(1)	2.677(1)	–B(3)	1.843(1)	1.844(1)
–2B(4)	2.707(1)	2.708(1)			
–2B(4)	2.760(1)	2.771(1)	B(2)–2B(5)	1.754(1)	1.755(1)
–2B(1)	2.810(1)	2.815(1)	–B(3)	1.806(1)	1.800(1)
–2B(5)	2.822(1)	2.830(1)	–B(2)	2.037(2)	2.041(2)
–2B(4)	2.902(1)	2.913(1)			
–2B(1)	3.043(1)	3.037(1)	B(3)–2B(5)	1.791(1)	1.791(1)
–RE	3.170(1)	3.159(1)	–2B(4)	1.794(1)	1.797(1)
–2B(1)	3.296(0)[b]	3.306(1)	–B(2)	1.806(1)	1.800(1)
–2RE	3.403(0)[b]	3.405(0)[b]	–B(1)	1.843(1)	1.844(1)
–Al	3.469(0)[b]	3.470(0)[b]			
–Al	3.583(0)[b]	3.591(0)[b]	B(4)–B(4)	1.776(1)	1.776(1)
–RE	3.642(1)	3.658(1)	–B(5)	1.788(1)	1.796(1)
			–B(3)	1.794(1)	1.797(1)
Al–4B(2)	2.051(1)	2.049(1)	–B(1)	1.800(1)	1.803(1)
–4B(3)	2.321(1)	2.320(1)	–B(5)	1.823(1)	1.821(1)
–4B(5)	2.438(1)	2.438(1)	–B(4)	1.863(2)	1.865(2)
–4B(1)	2.861(1)	2.866(1)			
–2Al	2.910(0)[b]	2.911(0)[b]	B(5)–B(2)	1.754(1)	1.755(1)
–4B(4)	3.339(1)	3.340(1)	–B(3)	1.791(1)	1.791(1)
–2RE	3.469(0)[b]	3.470(0)[b]	–B(4)	1.788(1)	1.796(1)
			–B(4)	1.823(1)	1.821(1)
			–B(1)	1.827(1)	1.828(1)
			–B(5)	1.818(1)	1.828(1)

[a] Not occurring in the structure owing to low occupancy.
[b] Indicates that $\sigma < 0.0005$ Å.

and the standard deviations, given below in parentheses, were estimated using the formula $\Sigma_i(x_i - \bar{x})^2/(n-1)$. The compositions of the two phases as determined by electron microprobe were $Y_{0.60(2)}Al_{0.62(1)}B_{14}$ and $Er_{0.61(2)}Al_{0.71(3)}B_{14}$. This should be compared with the compositions obtained from the structure refinements, $Y_{0.620(2)}Al_{0.708(3)}B_{14}$ and $Er_{0.620(2)}Al_{0.732(4)}B_{14}$ respectively (the estimated standard deviations are given in parentheses). The agreement is good with the exception of the aluminium content of the yttrium compound, for which the microprobe analysis gives a lower value than the structure refinement, although on the limit of significance. However, we regard the occupancy values from the refinements as more reliable than the concentration values from the electron microprobe analyses.

4. Discussion

The crystal structure of $MgAlB_{14}$ [4, 11] and that of the closely related structure of NaB_{15} [12] ($NaBB_{14}$) were determined as early as 1970. Diffraction studies of other representatives of the $MgAlB_{14}$-type structure have subsequently been undertaken and the structure type has been described in various reports [13]. Therefore only a very general description is presented in the present paper.

The structure (a stereopair is shown in Fig. 1) can be described in terms of a rigid three-dimensional network of slightly deformed boron icosahedra (boron atoms B(1) and B(3)–B(5)), which are interconnected via external B–B bonds or via non-icosahedral boron atoms (B(2)). The metal atoms are accommodated in two types of interstitial hole situated between the icosahedra. The aluminium atoms partially occupy a chain of holes extending in the *a* direction. The holes have their centres at a distance of *a*/2 (*i.e.* 2.91 Å) from each other. The rare earth atoms partially occupy a zigzag chain of holes also extending in the *a* direction at a distance of approximately 3.16 Å from each other. In both cases the distances between the holes along the chains are close to the metal–metal distance of the elements. Both metal positions are only partially occupied, a feature that was also found in

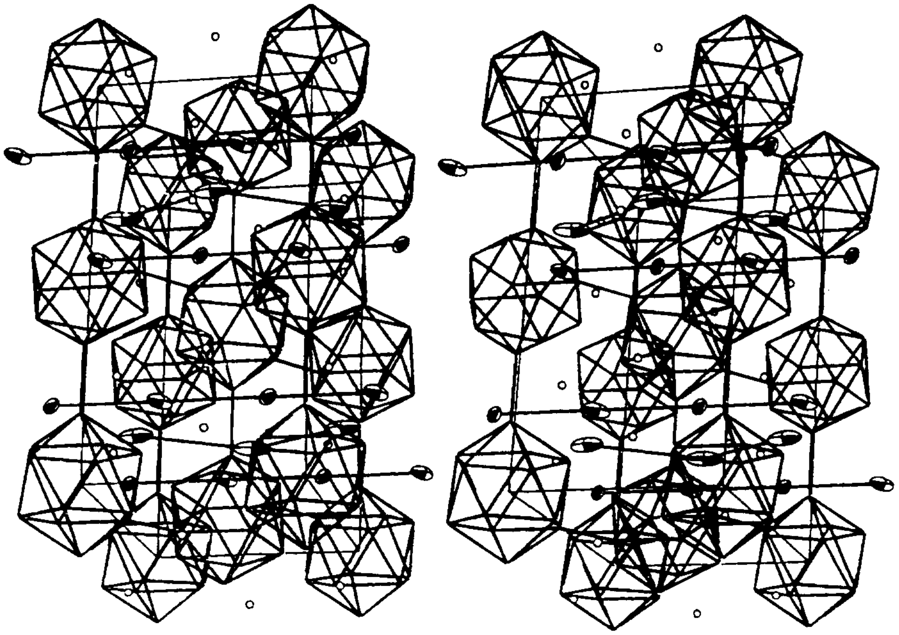

Fig. 1. A simplified stereo pair of the crystal structure of $Er_{0.62}Al_{0.73}B_{14}$. The *a* axis is horizontal, the *b* axis vertical and the *c* axis penetrating the figure. Small open circles denote non-icosahedral B(2) atoms, which are not connected with their neighbours via bond bars. The thermal ellipsoids of erbium form zigzag chains in the *a* direction while those of aluminium form straight lines in the same direction.

$Mg_{0.78}Al_{0.75}B_{14}$ [5] and in $Ho_{0.63}Al_{0.74}B_{14}$ [1]. The reader is referred to ref. 5 for a detailed discussion of the environment of the metal atoms.

From the interatomic distances in Table 5 it can be seen that aluminium is accommodated in the smaller hole at an average distance of 2.27 Å from its 12 boron neighbours, while the rare earth atoms are situated at an average distance of 2.72 Å from their 16 boron neighbours with individual distances scattered between 2.41 and 2.90 Å. The very short four Al–B(2) distances of 2.05 Å in both structures investigated is noticeable. This distance is very much shorter than the neutral atomic radius sum of 2.33 Å. This short distance has already been noticed in $LiAlB_{14}$ and $MgAlB_{14}$ by Higashi [4] and support his conclusion that the metal atoms bond more strongly to the isolated non-icosahedral boron atoms (B(2)) than to the icosahedral boron atoms.

A new feature of the present structures is the occurrence of a significant splitting of the 4e position (site symmetry, $mm2$). Such a splitting was not observed in $Ho_{0.63}Al_{0.74}B_{14}$ [3]. However, in our refinements we did not obtain low agreement indices until the rare earth atoms were assigned to the 8i position (site symmetry, m) which is about 0.14 Å from the mirror plane perpendicular to the a axis. This means that there is a static disorder in the hole accommodating the rare earth atoms: the rare earth atom is randomly distributed in different unit cells among positions with $+x$ and $-x$ coordinates of the 8i position. The shortest RE–RE distances (RE ≡ rare earth) (see Table 5), of course, never occur in the structure because at the low occupancy of the position. It should also be noted that the split rare earth position in Fig. 1 is presented only as one thermal ellipsoid, which thus represents the static disorder as well as the thermal vibrations. A closer analysis shows that the thermal vibrations extend anisotropically in the a direction and that there are fewer nearest neighbours in this direction than perpendicular to it. However, the main contribution to the thermal ellipsoid comes from static disorder of the split position 4e. A similar splitting of the 4e position was earlier reported for a non-rare earth compound, namely $Mg_{0.78}Al_{0.75}B_{14}$ itself [5].

In a recent charge density study on $LiAlB_{14}$, Ito and Higashi [14] suggested that this structure is stabilized by a charge transfer from the metal atoms to the electron-deficient boron network. The experimental determination of the degree of charge transfer is, however, very difficult and the Ito and Higashi arrived at a net charge distribution of $Li^{+}(Al^{1.7+})_{0.96}$ using the method of population analysis of valence electrons, while a net charge distribution of $Li^{0.7+}Al^{1.5+}$ was obtained using the method of charge integration around the metal atoms. In this context it is interesting to analyse the number of valence electrons available for charge transfer in compounds crystallizing in the $MgAlB_{14}$-type structure considering partial occupancies of the metal positions. The data have been collected in Table 6. It is apparent that the number of valence electrons available for charge transfer is very close to four for all compounds considered, although different occupancies and valencies occur. For the lithium compound, however, the experi-

TABLE 6

Valence electrons available for stabilization of the three-dimensional boron network in $MgAlB_{14}$-type structures

Compound	Number of electrons	Reference
$LiAlB_{14}$	3.87	[4]
$Mg_{0.78}Al_{0.75}B_{14}$	3.81	[5]
$Mg_{0.93}MgB_{14}$	3.86	[15]
$Y_{0.62}Al_{0.71}B_{14}$	3.99	This paper
$Ho_{0.63}Al_{0.74}B_{14}$	4.11	[3]
$Er_{0.62}Al_{0.73}B_{14}$	4.05	This paper

mentally determined charge transfer was considerably lower, namely 2.2–2.6 electrons.

Finally, it is noted that a splitting of a similar type as that found for the rare earth position in the present study was established for a number of solid state ionic compounds and some other compounds with unusual physical properties [16]. The observed rare earth site splitting and positional disorder clearly indicate new trends in the studies of physical properties of the present materials, which are far from being thoroughly investigated as yet.

Acknowledgments

The authors are indebted to Dr. Claes Åhlinder, Geological Survey of Sweden, Uppsala, for microprobe analyses. The financial support of the Swedish Board for Technical Development and the Swedish Natural Science Research Council is gratefully acknowledged. One of us (M.K.) wishes to express her gratitude to the whole staff of the Inorganic Chemistry Department for the friendly atmosphere during her stay.

References

1. Yu. B. Kuz'ma, V. N. Gurin, M. M. Korsukova, N. F. Chaban and S. I. Chikhrij, *Izv. Akad. Nauk SSSR, Neorg. Mater.*, *24* (1988) 1705.
2. N. B. Brandt, A. A. Gippius, V. V. Moshchalkov, K. K. Nyan, V. N. Gurin, M. M. Korsukova and Yu. B. Kuz'ma, *Sov. Phys.–Solid State*, *30* (1988) 797.
3. M. M. Korsukova, V. N. Gurin, Yu. B. Kuz'ma, N. F. Chaban, S. I. Chikhrij, V. V. Moshchalkov, N. B. Brandt, A. A. Gippius and K. K. Nyan, *Phys. Status Solidi A*, *114* (1989) 265.
4. I. Higashi, *J. Less-Common Met.*, *82* (1981) 317.
5. I. Higashi and T. Ito, *J. Less-Common Met.*, *92* (1983) 239.
6. J.-O. Lungren (ed.), Crystallographic computer programs, *UUIC Publ. B18-4-5*, 1982 (Institute of Chemistry, University of Uppsala).
7. P. Becker and P. Coppens, *Acta Crystallogr. Sect. A*, *30* (1974) 129; *31* (1975) 417.
8. J. A. Ibers and W. C. Hamilton (eds.), *International Tables for X-ray Crystallography*, Vol. IV, Kynoch Press, Birmingham, 1974.

9 T. Hahn (ed.), *International Tables for X-ray Crystallography*, Vol. I, Reidel, Dordrecht, 1983.

10 E. D. Stevens and P. Coppens, *Acta Crystallogr., Sect. A, 32* (1976) 915.

11 V. I. Matkovich and J. Economy, *Acta Crystallogr., Sect. B, 26* (1970) 616.

12 R. Naslain and J. S. Kasper, *J. Solid State Chem., 1* (1970) 150.

13 R. Naslain, in V. I. Matkovich (ed.), *Boron and Refractory Borides*, Springer, Berlin, 1977, pp. 139–202.

14 T. Ito and I. Higashi, *Acta Crystallogr., Sect. B, 39* (1983), 239.

15 A. Guette, M. Barret, R. Naslain, P. Hagenmüller, L.-E. Tergenius and T. Lundström, *J. Less-Common Met., 82* (1981) 325.

16 V. B. Kalinin and A. M. Golubev, *Sov. Phys.-Crystallogr., 35* (1990) 867.